

X-ray microdiffraction study of Cu interconnects

X. Zhang,^{a)} H. Solak, and F. Cerrina

*Electrical and Computer Engineering Department and Center for Nanotechnology,
University of Wisconsin–Madison, Madison, Wisconsin 53706*

B. Lai, Z. Cai, P. Ilinski, D. Legnini, and W. Rodrigues

Advanced Photon Source, Argonne National Laboratory, Argonne, Illinois 60439

(Received 30 September 1999; accepted for publication 22 November 1999)

We have used x-ray microdiffraction to study the local structure and strain variation of copper interconnects. Different types of local microstructures have been found in different samples. Our data show that the Ti adhesion layer has a very dramatic effect on Cu microstructure. Strain measurement was conducted before and after electromigration test, Cu fluorescence was used to find the mass variations around voids and hillocks, and x-ray microdiffraction was used to measure the strain change around that interested region. © 2000 American Institute of Physics.

[S0003-6951(00)03903-6]

Reliability is a key issue in integrated circuit (IC) performance, and interconnect failure has been in the forefront of reliability issues for integrated circuits for the last two decades.^{1,2} In general, electromigration and mechanical stress related damages have been identified as the major causes for these interconnect failures in aluminum conductors.^{3,4} Copper is the major candidate to replace aluminum alloys as the interconnect material for advanced ICs,^{5–8} because it has lower resistivity and higher resistance against electromigration failure.

Electromigration is the movement of atoms caused by flow of electrons. The phenomenon is attributed to the momentum transfer from electrons to atoms or *electron wind force*.³ High current densities (10^5 A/cm²) may cause substantial mass transport, thus creating microvoids that eventually may cause open circuit failure. It is also well known that electromigration is strongly influenced by the mechanical stress that exists in interconnects.⁴ When the migration of atoms happens, material is accumulated in some places (usually close to the anode) and depleted in other places (close to the cathode). This movement of material induces a stress field in the lines that are confined by the substrate and passivation layer. In return, the stress field creates a force against the electromigration. Under certain conditions, these two forces can balance each other and the electromigration will stop. Thus, understanding the role of stress, and hence strain, in electromigration is essential.

Many models have been developed to predict the evolution of stress in interconnects due to electromigration.^{9–13} However, experimental verification is very difficult mainly because of the challenge of stress measurement in the extremely small volumes of lines with micron or submicron spatial resolution. In addition, interconnect lines must be studied in a realistic IC environment, thus limiting the applicability of surface sensitive techniques^{14,15} since the complex structure requires a probe capable of penetrating several microns of dielectrics while maintaining a good spatial resolution. X-ray diffraction is a direct technique for strain mea-

surement and has been successfully used for detailed characterization of average strain in interconnect lines. However, the area sampled with traditional x-ray diffraction tools is too large to allow measurement of strain distribution with the required spatial resolution. The development of x-ray microdiffraction has opened new possibilities in this area.^{16–18} In these experiments, the photon density at the sample is increased to a level sufficient to acquire diffraction data from extremely small volume, such as $0.3 \mu\text{m}^3$. In this letter, we report the application of this state of art x-ray microbeam diffraction technique to the study of electromigration and stress phenomena causing reliability problems in Cu interconnects.

The copper interconnect structures were fabricated using a lift-off process. After applying APEX-E photoresist on thermally oxidized Si wafers, electron beam lithography was used to directly write the patterns. Eight different linewidths were used in this experiment, varying from $5 \mu\text{m}$ to $0.25 \mu\text{m}$. The length of all lines was 1 mm. After the photoresist development, an electron beam evaporator was used to deposit Cu (350 nm) or Cu (350 nm)/Ti (20 nm) films on these wafers, Ti being used as an adhesion and barrier layer.^{19,20} An ultrasonic bath was then used to resolve the interconnect patterns. SiN ($0.2 \mu\text{m}$) and SiO ($0.4 \mu\text{m}$) were deposited as the top passivation layers using plasma-enhanced chemical vapor deposition (PECVD) at 350°C . Conventional optical lithography was used to open the contact holes, and Al was evaporated on the samples as the outside contact metal. Hence, the copper interconnects were completely buried in the glass passivation layer. Finally, the wafers were annealed at 450°C for 30 min in a $\text{N}_2(90\%)/\text{H}_2(10\%)$ mixture.

The x-ray microdiffraction experiments were conducted at Argonne National Laboratory, on beamline 2ID-D. The optical layout and performances are described in Refs. 17 and 18; it has demonstrated a resolution of $0.2 \mu\text{m}$, with an efficiency of 40% in the first order focus. In our experiment we use a spot of $1 \times 5 \mu\text{m}^2$ at a photon energy of 9.5 keV. In this experiment, we used symmetric reflection geometry with the incident and reflected beams making approximately the same angle with the surface normal. Therefore, the strain

^{a)}Electronic mail: xzhang@xraylith.wisc.edu

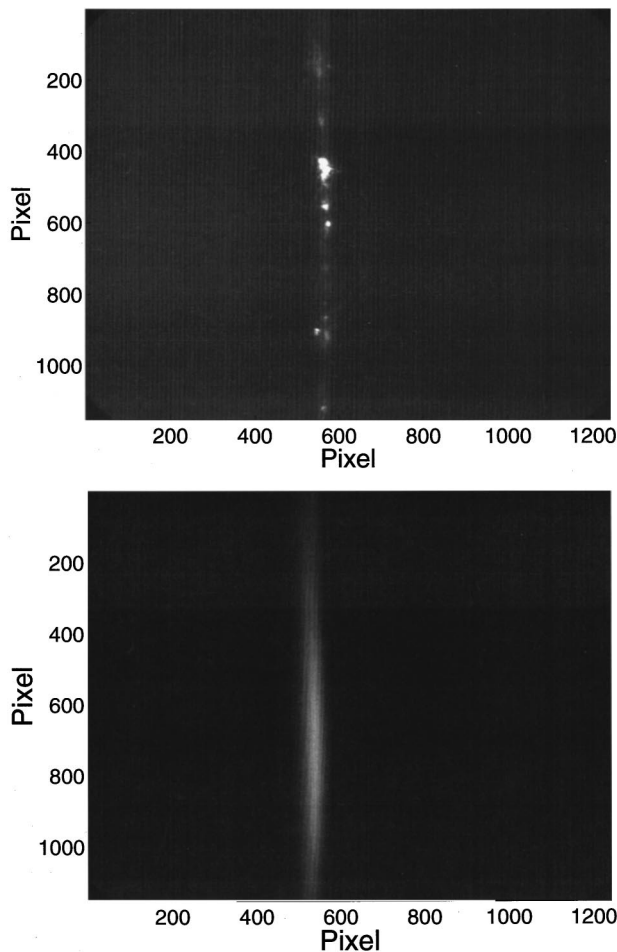


FIG. 1. Diffraction patterns from different interconnect samples.

measurements of our experiment are sensitive only to the surface normal direction. In order to position the sample area of interest in the microbeam, an energy-dispersive Germanium detector was used to detect the copper $K\alpha$ (8.0 keV) fluorescence. By scanning the sample in both horizontal and vertical directions and knowing the exact geometry of the pattern on the sample, we were able to accurately locate the microbeam and repeatably place the area of interest under it. An x-ray charge coupled device (CCD) camera on the 2θ arm of the goniometer was used to record the diffraction patterns from the sample. A typical example is shown in Fig. 1; the data files are in the format of 16 bit 1152×1242 gray-scale images. In our experiment, we used $E = 9.5$ keV photon energy to obtain the diffraction from a given family of lattice planes.

Our experimental results show that the Ti adhesion layer has a dramatic effect on the microstructure of the Cu film deposited on top. As-deposited pure Cu film showed typical polycrystalline structure and in our experiment, we found diffraction spots from (111), (200), (220), (311), and (222) plane families at θ angles equal to 18.25° , 21.19° , 30.75° , 36.85° , and 38.77° . According to the atomic force microscopy (AFM) data, the as-deposited pure Cu film has initially a grain size about $0.15 \mu\text{m}$ and increasing to $0.4 \mu\text{m}$ after annealing, which is very close to its thickness. A subset of the x-ray diffraction patterns is shown in Fig. 1, limited to the case of the (111) plane family of pure Cu film and Cu/Ti bilayer. Only a few grains are located within the focused

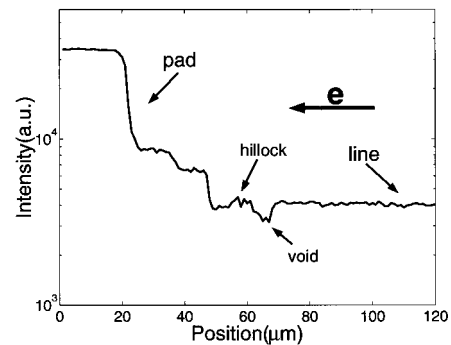


FIG. 2. Cu fluorescence scan along a $2 \mu\text{m}$ line after electromigration test.

beam, and the top panel of Fig. 1 shows the corresponding diffraction spots. In the samples with the Ti adhesion layer (Fig. 1, lower panel), we observe a broader image than expected from a distribution of smaller grains; we found that the film has strong (111) texture. We observe that the width of the x-ray diffraction spot is consistent with a grain size of about 40 nm . In addition, we were not able to find any diffraction from other plane families from this Cu/Ti film. The sample has a 30 min 450°C annealing history. The microstructures of Cu/Ti bilayers have been investigated by several researchers;^{21,22} various textures and grain sizes have been reported, ranging from 0.03 – $0.15 \mu\text{m}$ before to 0.05 – $0.4 \mu\text{m}$ after annealing, depending on the process.²³

The electromigration test was conducted on the Cu/Ti sample at 250°C and about $7.8 \times 10^6 \text{ A/cm}^2$. After 52 h electrical stressing, the total current had reduced to $\sim 6\%$ of its original value, indicating that electromigration had damaged most of the test patterns. Combining optical microscope and Cu fluorescence, we could easily find the region of interest. In Fig. 2, we show the fluorescence signal from Cu along one single $2 \mu\text{m}$ line. The spatial resolution is $1 \mu\text{m}$. Since the intensity of this Cu fluorescence is proportional to the mass of the Cu under the x-ray beam spot, different features can be identified in this scan. The anode contact pad extending from 0 to about $25 \mu\text{m}$ gives the strongest signal. The variation of intensity from 25 to $70 \mu\text{m}$ shows the Cu depletion and Cu accumulation along the line, and a much more uniform intensity can be found after that region. The scan shows the existence of an upstream void and a downstream hillock.

An x-ray microdiffraction scan was then conducted around this area. The step sizes were 1 and $4 \mu\text{m}$. In Fig. 3 we show the method we used to calculate the strain and the results of the strain variation along the same $2 \mu\text{m}$ line before and after electromigration. It should be noted that our major concern in this experiment was to profile the strain distribution along the line rather than obtaining an absolute measurement. In the top panel of Fig. 3, we show a composite of the typical diffraction pattern from our experiment, together with the best fit to the diffraction arc. The average relative strain of that spot $\Delta\epsilon$ is calculated by comparison of the center of this arc to a reference $\Delta\epsilon = \Delta n/2r \tan \theta$, where Δn is the difference between the two arcs in pixel number, s is the size of pixel which is $50 \mu\text{m}$ in our case, r is the distance between the sample and the CCD camera which is 64.38 cm , and θ is the Bragg angle. Hence, we obtain an instrumental sensitivity of

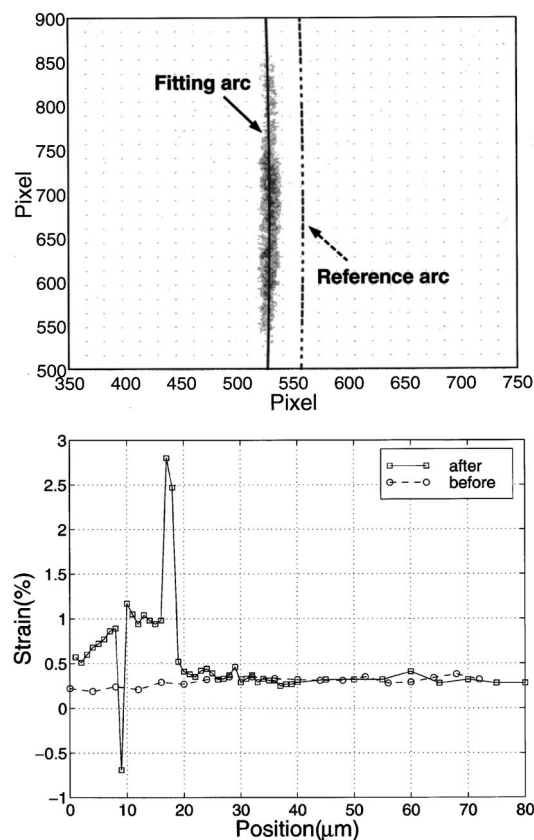


FIG. 3. Data analysis and strain calculation.

$$\frac{\Delta \epsilon}{\Delta n} = \frac{50}{2(64.38 \times 10^4) \tan(18.25^\circ)} \sim 1.2 \times 10^{-4} \text{ pixels}^{-1}.$$

In this experiment, we chose the diffraction arc from the 1 mm by 1 mm Cu contact pad as the reference. It should be noted that although a Cu contact pad may not be stress free, its stress will be much lower than that of the more constrained lines.

In the low panel of Fig. 3, we show the final calculation results of the strain variation along the same 2 μm line before and after electromigration. Comparing Figs. 2 and 3, we conclude that the region we scanned in Fig. 3 is the region starting from about 40 μm and beyond in Fig. 2. Significant strain variation around the void and hillock has been found. From our data, we found that there is a very large tensile-like deviation around the void which may not be explained as a tensile strain in copper. We believe that the diffraction is actually from the TiCu alloy formed during annealing process. Liotard *et al.*²³ have done extensive studies on Cu/Ti bilayer using different methods and have shown that various CuTi alloys can be formed at the interface between Cu and Ti during the high temperature process. Our energy dispersive spectroscopy (EDS) data also show that there is a higher Ti peak at the void area, indicating that there is a significant amount of CuTi left in the void. The strain goes to compressive around the hillock, which is close to the anode. Recently, Wang *et al.*²⁴ have shown that compressive stress gradient builds up during the electrical stressing procedure and relaxes quickly after the stressing is stopped on a 10 μm Al strip. In our experiment, the relaxation path was severed by the void and the compressive strain remained unchanged around the hillock long after the electrical stressing stopped.

Figure 3 also shows that the average strain has no significant difference beyond the void in the two different conditions, which is consistent with this stress relaxation mechanism.

In conclusion, in this letter we report microdiffraction data from Cu interconnects. The results show that x-ray microdiffraction and microfluorescence can provide important insights in electromigration studies. In our experiment, we found that the 20 nm Ti adhesion layer can significantly change the microstructure of Cu film deposited on top of it. The as-deposited Cu film did not show any preferred orientation, but the Cu/Ti film showed strong (111) texture and fine grains. The microdiffraction experiment was conducted before and after the electromigration test. Significant mass flow and strain variation were found along the same line after electrical stressing. Large compressive strain was found around the hillock area, while the TiCu alloy complicated the stress state analysis around the void region. We did not observe any changes in the area far from the damage region, meaning that the stress relaxation in that region was quite fast. It can be very interesting to extend our studies to include *in situ* microdiffraction measurements to investigate the stress evolution during the electrical stressing. We are also extending our studies to other interconnect structures, such as Ta/Cu/Ta and TiN/Cu/TiN.

This project is supported by the Advanced Photon Source under Contract No. PO 062242-02. The Center for Nanotechnology is supported by DARPA under Grant No. N00014-97-1-0460.

- ¹J. Curry, G. Fitzgibbon, Y. Guan, R. Muollo, G. Nelson, and A. Thomas, Proceedings of the 20th Annual International Reliability Symposium, 1984, p. 6.
- ²J. Klema, R. Pyle, and E. Domangue, Proceedings of the 22nd Annual International Reliability Symposium 1984, pg. 1.
- ³R. S. Sorbello, Mater. Res. Soc. Symp. Proc. **225**, 3 (1991).
- ⁴I. A. Blech, J. Appl. Phys. **47**, 1203 (1976).
- ⁵C. K. Hu and J. M. E. Harper, International Symposium on VLSI Technology and Applications, 1997, pp. 18–22.
- ⁶D. Gupta, Mater. Chem. Phys. **41**, 199 (1995).
- ⁷D. B. Knorr and D. P. Tracy, Mater. Chem. Phys. **41**, 206 (1995).
- ⁸J. Li, T. E. Seidel, and J. W. Mayer, MRS Bull. **19**, 15 (1994).
- ⁹M. A. Korhonen, P. Borgesen, K. N. Tu, and C. Li, J. Appl. Phys. **73**, 3790 (1993).
- ¹⁰C. L. Bauer and W. W. Mullins, Appl. Phys. Lett. **61**, 2987 (1992).
- ¹¹R. J. Gleixner and W. D. Nix, J. Appl. Phys. **83**, 3595 (1998).
- ¹²Y. J. Park and C. V. Thompson, J. Appl. Phys. **82**, 4277 (1997).
- ¹³Y. Liu, C. L. Cox, and R. J. Diefendorf, J. Appl. Phys. **83**, 3600 (1998).
- ¹⁴S. Singh, H. Solak, N. Krasnoperov, F. Cerrina, A. Cossy, J. Diaz, J. Stohr, and M. Samant, Appl. Phys. Lett. **71**, 55 (1997).
- ¹⁵H. Solak, G. F. Lorusso, S. Singh, and F. Cerrina, Appl. Phys. Lett. **74**, 22 (1999).
- ¹⁶W. Yun, B. Lai, D. Shu, A. Khounsary, Z. Cai, J. Barraza, and D. Legnini, Rev. Sci. Instrum. **67**, 3373 (1996).
- ¹⁷B. Lai, W. Yun, D. Legnini, Y. Xiao, J. Chrzas, P. Viccaro, V. White, S. Bajjkar, D. Denton, F. Cerrina, E. Fabrizio, M. Gentili, L. Grella, and M. Baciocchi, Appl. Phys. Lett. **61**, 1877 (1992).
- ¹⁸H. H. Solak, Y. Vladimirovsky, F. Cerrina, B. Lai, W. Yun, Z. Cai, P. Ilinski, D. Legnini, and W. Rodrigues, J. Appl. Phys. **86**, 884 (1999).
- ¹⁹S. W. Russell, S. A. Rafalski, R. L. Spreitzer, J. Li, M. Moynour, F. Moghadam, and T. L. Alford, Thin Solid Films **262**, 154 (1995).
- ²⁰S. Q. Wang, MRS Bull. **19**, 30 (1994).
- ²¹D. P. Tracy, D. B. Knorr, and K. P. Rodbell, J. Appl. Phys. **76**, 2671 (1994).
- ²²R. Frankovic and G. H. Bernstein, Mater. Res. Soc. Symp. Proc. **391**, 403 (1995).
- ²³J. L. Liotard, D. Gupta, P. A. Saras, and P. S. Ho, J. Appl. Phys. **57**, 1895 (1985).
- ²⁴P.-C. Wang, G. S. Cargill, I. C. Noyan, and C.-K. Hu, Appl. Phys. Lett. **72**, 1296 (1998).